INTERNATIONAL JOURNAL OF AUTOMOTIVE AND MECHANICAL ENGINEERING (IJAME)
ISSN: 2229-8649 e-ISSN: 2180-1606
VOL. 19, ISSUE 4, 2022, 10103 – 10111
DOI: https://doi.org/10.15282/ijame.19.4.2022.07.0781

ORIGINAL ARTICLE

Effect of Tool Shoulder-to-Pin Diameter Ratio (D/d) on the Mechanical Properties of Friction Stir Processed Mg-Micro Al_2O_3 Composite

M. R. A. Mohd Reduan[1], Z. Zulkfli[1,*], Z. Hamedon[1] and N. Fatchurrohman[2]

[1]Faculty of Manufacturing and Mechatronic Engineering Technology, Universiti Malaysia Pahang, 26600 Pahang, Malaysia
[2]Department of Industrial Engineering, Faculty of Engineering, Universitas Putra Indonesia YPTK, Padang 25221, Indonesia

ABSTRACT – The engineering industry uses magnesium as it is a low density to lightweight ratio material and able to replace the heavier material. Friction stir processing is an applicable method to modify the structural properties of the workpiece. H13 steel tools are produced into several tool parameters with different shoulder diameters to pin diameters (D/d) ratios. A fixed machining parameter of 1040 rpm for spindle speed and 17 mm/min for traverse speed was used throughout this study. Contact between the tool and workpiece produces frictional heat that softens the material. By creating magnesium alloys into metal matrix composites (MMC), microsized aluminum oxide powder (Al_2O_3) was reinforced during FSP to enhance the mechanical properties of the magnesium alloy AZ91A. The aim of this study is to analyze and obtain the optimal tool parameter to process Mg-Micro Al2O3. The microstructure of FSPed Mg-Micro Al_2O_3 was observed using a light microscope, specifically on the grain size. The hardness test was done utilizing the Rockwell Hardness Tester to validate the changes in the hardness. The shoulder diameter of 12 mm was found to be the most suitable parameter for processing Mg-Micro Al_2O_3 as it produced fewer defects and finer grain size.

ARTICLE HISTORY
Received: 15th Mar. 2022
Revised: 16th June 2022
Accepted: 13th Dec. 2022
Published: 28th Dec. 2022

KEYWORDS
Friction stir processing;
Magnesium alloy AZ91A;
Aluminium oxide;
(D/d) ratio;
Mechanical properties

INTRODUCTION

High demand in automotive and aircraft fabrication to reduce weight urges the usage of low-weight materials in optimizing the products' design in order to obtain efficient energy consumption as well as can improve passenger safety [1]. Therefore, lighter metals such as magnesium alloys are highly desirable in replacing conventional materials. However, the strength of magnesium alloys is not sufficient and their reinforcement is needed. Magnesium-based metal matrix composite (MMC) are suitable for such applications due to the matrix's high strength and ductility of hard reinforcing particles. Due to the strength-to-weight ratio as well as high specific modulus, fatigue strength and wear resistance, magnesium alloys become an attraction in this industry [2]-[4].

The basic principle of friction stir processing (FSP) was originally developed from friction stir welding (FSW), which is currently used as a potential mechanism to modify the microstructure of metallic material [5]. FSP is considered to be the most suitable method to produce finer and even particles of alloy matrix. The method is efficient as it uses the localized heat generated by friction from contact between a rotating non-consumable cylindrical tool and workpiece. The friction leads to the local temperature increment, hence modifying the material's properties [6], [7]. The designed tool rotated at high speed and traversed along the workpiece with a specific length and speed. The material is expelled around the tool before being forged downward by a great load. Grain will be refined significantly as the material undergoes intense plastic deformation during this process [8]. Besides the attractive mechanical properties, FSP offers cost and weight savings [9].

Generally, the process parameters such as the type of material and depth of tool penetration have a big impact on fabricating composites. The selection of tool rotating speed and traverse speed is also important to ensure sufficient heat generation on the workpiece during FSP [10]. The tool design plus the tool shoulder diameter and pin control heat generation and could improve grain properties. Further, the tool geometry, such as shoulder diameter as well as the pin shape [11], size and feature [12], [13], alters the plasticized material flow. The tool shoulder and pin combination affects heat generation and material flow, impacting particle distribution and the microstructure [14]. The tool shoulder is responsible for the material flow, whereas the tool pin facilitates the material flow layer-by-layer.

Mg-Al usage is common in the automotive industry, but the metal matrix composites resulting from stir casting lead to uneven distribution of reinforcement particles which affects the quality of the composite. In the industry application, selecting the most suitable tool parameters are important for future implementation. Severe plastic deformation by FSP is an effective technique for obtaining high-strength ultrafine-grain microstructure [15]. Shoulder diameter to pin diameter ratios (D/d) of the tool is crucial as the tool parameter influences the final results of the friction stir processed (FSPed) zone. The effect of using different tool pin shapes and different welding parameters using a constant rotational speed was compared [16]. To the authors' best knowledge, no study comparing the shoulder-to-pin diameter ratio, especially on this alloy, has been presented before. This study aims to fabricate practical tools with selected tool parameters that signify the mechanical properties and microstructure of the FSPed material, to overcome the uneven distribution of the reinforcement

*CORRESPONDING AUTHOR | Z. Zulkfli | ✉ zulkflizuhairah@gmail.com

problem and the capability of the FSPed zone properties [17]. The effect of different shoulder-to-pin diameter ratios on the hardness and microstructure of Mg-Micro Al_2O_3 MMC was analyzed. To obtain desired results, the parameters must be fixed at a specific standard and taken control throughout this study.

The remainder of this paper is classified as follows; section 2 briefly presents the step-by-step procedure from providing the experimental settings to preparing samples, section 3 explains the macrostructure and microstructure observations of Mg-Micro Al_2O_3 as well as hardness values achieved after modification and section 4 concludes the paper.

EXPERIMENTAL METHOD

In this experiment process, the material used for the FSP tools is the H13 steel rod. Several FSP tools were fabricated using the lathe machine consisting of two main parts, which are the shoulder and pin, shown in Figure 1. The material used in FSP for workpieces is magnesium alloy AZ91A. The workpiece was prepared into some samples by using the Makino KE55 milling machine**.** Five variations of the shoulder (D) to pin (d) diameter ratio, (D/d) shown in Table 1 were designed as the tool parameters used in this study. The tool parameter that changes are the diameter of the shoulder (D), while the diameter of the pin (d) was fixed at 6 mm with a length (l) of 3 mm. The body diameter for each FSP tool was 20 mm whereas the length of the shoulder (L) is 15 mm. The general mechanical properties of the H13 steel tool and the workpiece used throughout this study which is magnesium AZ91A alloy are tabulated in Table 2.

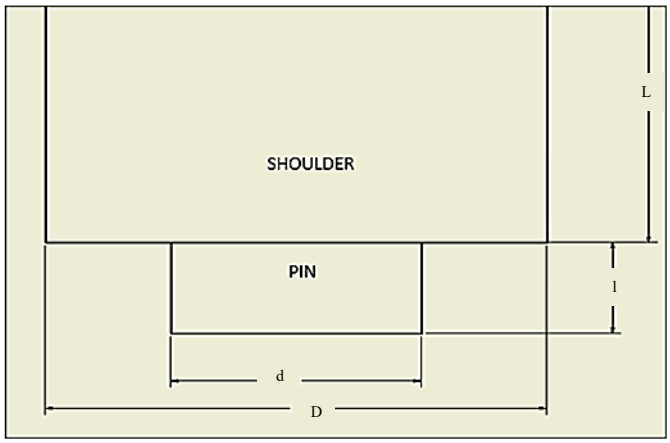

Figure 1. FSP tool schematic drawing

Table 1. FSP tool parameters

No	Shoulder diameter, D (mm)	Pin diameter, d (mm)	Shoulder to pin diameter ratio, D/d
1.	9	6	1.50
2.	12	6	2.00
3.	15	6	2.50
4.	18	6	3.00
5.	20	6	3.33

Table 2. Properties of magnesium AZ91A alloy

Material Properties	H13 Steel	Mg AZ91A
Young's modulus (GPa)	210	44.80
Poisson's ratio	0.30	0.35
Tensile strength (MPa)	1990	230
Yield strength (MPa)	1650	150
Density (kg/m^3)	7835	1810
Thermal conductivity (W/mK)	28.60	72.70
Melting temperature (K)	1745	694.15

In addition, the chemical composition of Mg AZ91A alloy is tabulated in Table 3. The major constituents of this alloy are aluminium and zinc, with weight percentages of 9% and 1%, respectively. Aluminium widens the freezing range and eases the casting process for the alloy. It also provides strength and hardness. On the other hand, zinc enhances oxidation resistance [18]. The other small constituents of magnesium AZ91 alloy are manganese (Mn), silicon (Si), iron (Fe), copper (Cu) and nickel (Ni). The magnesium alloy AZ91A block with an actual size of 170×52×52 mm was cut and prepared into five smaller blocks of 22 mm in length each. Then, each of the blocks undergoes squaring process to achieve a dimension of 51×51×21 mm as shown in Figure 2.

Table 3. Chemical composition of magnesium AZ91A alloy

Element	Al	Zn	Mn	Si	Fe	Cu	Ni	Mg
Composition (wt.%)	9.0	1.0	0.5	0.1	0.005	0.003	0.002	Remaining

An alternative procedure to fabricate surface composite is by preparing a hole or cutting a groove along the direction of FSP filled by the reinforcement. The FSP tool will travel along the groove to create a thick layer of surface composite [19]. Therefore, four holes of diameter: 3 mm with 1.5 mm deep were made along the centreline of the workpiece. Aluminium oxide (Al_2O_3) powder was filled and compacted in these holes. Al_2O_3 particles with (≤10 µm average particle size) were used as the reinforced particles throughout the FSP experiments. The mechanical properties of the reinforced powder, Al_2O_3 shown in Table 4.

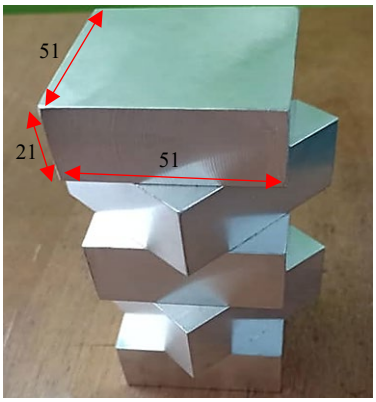

Figure 2. Magnesium alloy AZ91A blocks after squaring process

Table 4. Mechanical properties of aluminium oxide

Material Properties	Al_2O_3
Melting point (°C)	2072
Boiling point (°C)	2977
Hardness (GPa)	15-19 (9 on the Mohs scale)
Mechanical strength (MPa)	300-630
Compressive strength (MPa)	2000-4000
Thermal conductivity (W/mK)	20-30
Molecular mass (g/mol)	101.96
Density (g/cm^3)	3.95

The Mg AZ91A workpiece was clamped and the FSP tool was inserted into the milling spindle head, as shown in Figure 3, before beginning the experiment. The machining parameters used throughout this study are a spindle speed of 1040 rpm and a traverse speed of 17 mm/min, which those parameters are commonly used when friction stir processing magnesium alloys. During FSP, a single pass was applied throughout the experiments. The steps were repeated and applied to all the samples using five variations of the shoulder diameter size tool. After completing FSP experiments, samples will undergo (i) surface morphology, (ii) hardness testing and (iii) microstructure observations.

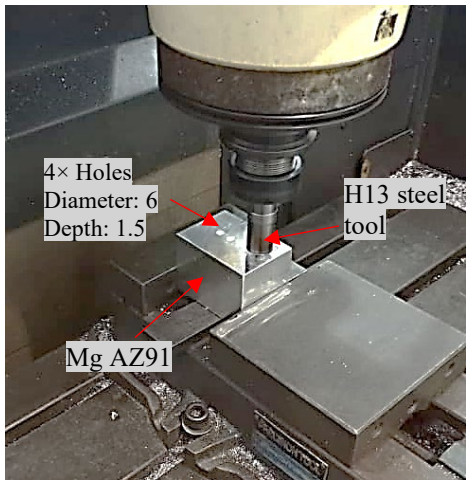

Figure 3. FSP tool and workpiece setup using the milling machine

After completing the surface morphology, the FSPed Mg-Micro Al_2O_3 workpieces will undergo hardness tests using Rockwell Hardness Tester CV-600A. Hardness tests measure the resistance of metal to plastic deformation against indentation, abrasion of cutting and scratching. The Rockwell hardness method was used to measure the hardness of the FSPed Mg AZ91A samples with reinforced particles through the depth of penetration of the indenter. This Rockwell hardness method is suitable for finished or machined parts of simple shapes. The Rockwell test requires no material preparation and the hardness value is easily readable without any extra equipment, making this one of the most commonly

used methods of measuring metal hardness. Furthermore, it is a faster and cheaper method when compared to Brinell and Vickers tests.

The workpieces will be placed directly on the Rockwell machine's table. Firstly, the hardness tester was set using the "B" scale with an initial force of 98.07 N which is known as minor load and 1.5875 mm-diameter ball indenter. The "B" scale is used for performing tests on soft steel, aluminium alloys, copper and malleable iron. The first minor load is applied to overcome the film thickness on the metal surface. Minor load also eliminates errors in the depth of measurements caused by the machine frame's spring or setting down of the specimen and table attachments. Then, the test can be proceeded by applying a force of 588.4 N on the Mg-Micro Al_2O_3 composite. This applied force was selected for the material type of magnesium alloy in the manual book of Rockwell Hardness Tester CV-600A.

Microscopic tests were conducted on the middle of each micro specimen to show the results on the mechanical properties of FSPed Mg-Micro Al_2O_3 focusing on the grain structure. The FSPed samples were prepared as following steps for the etching process; (1) cut into micro section specimens at the middle point of the processed zone, (2) micro-sectioned specimens were mounted using resin, (3) then, the specimens were ground using emery papers starting from 80 grits to 2500 grits and (4) polished using fine velvet cloth with 1-micron diamond paste solution following the standard metallographic technique, (5) specimens were etched via immersion for 3-5 seconds by using a glycol reagent which has a composition of 1 mL Nitric acid (HNO_3), 24 mL of distilled water and 75 mL of ethylene glycol, and (6) finally, specimens were rinsed and lastly dry [20]. Specimens are ready to be observed using LEXT^{TM} OLS5000 3D Laser Scanning Microscope for analysis.

RESULTS AND DISCUSSION

This study was mainly focusing on the surface morphology, hardness and microstructure of FSPed Mg AZ91A reinforced with Al_2O_3 particles. The action of the rotating tool shoulder assists in the occurrence of material flow on the top surface of the FSP zone. The shoulder influences the movement of the material at the upper one-third from the surface of the FSP zone rather than the pin profile [21], [22].

Surface morphology on FSPed Mg AZ91A/Al_2O_3

The first step for analysis is the surface morphology on the processed surface of FSPed Mg-Micro Al_2O_3 workpieces. The presentation of the workpiece, together with the defects, was observed and analyzed. Figure 4(a) indicates the FSPed Mg-Micro Al_2O_3 composite using a 20 mm-diameter tool shoulder. Heat input increases when using the large shoulder diameter of the tool, applying high rotational speed but low traverse speed. Due to bigger surface contact during FSP, heat generated due to friction is high [23], making a burnt mark on the stir zone. Another defect observed is tunnel defect on Mg-Micro Al_2O_3 due to low heat input, which leads to surface lack of fill since the material flow decreased [24], [25]. Figure 4(b) shows the observation using an 18 mm-diameter tool shoulder in which the stirred zone is shinier, indicating that the reinforced particles mixed in better with Mg AZ91A compared to FSPed Mg-Micro Al_2O_3 composite using a 20 mm-diameter tool shoulder. It is applicable that the tool shoulder diameter is important to enhance material flow and obtain adequate particle distribution [26]. However, there was also a tunnel defect on the surface. Next, Figure 4(c) displays the observation of FSP using a 15 mm-diameter tool shoulder which the FSP zone line on FSPed Mg-Micro Al_2O_3 composite is more stable as the tool shoulder produces better heat generation compared to the results when using 18 mm and 20 mm shoulder diameter but tunnel defect also occurred on the sample.

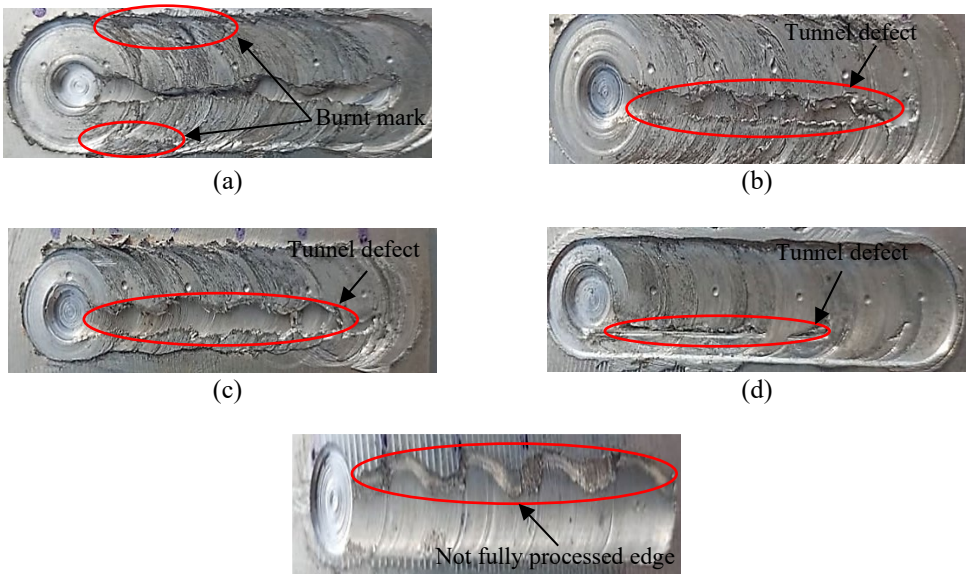

Figure 4. The surface morphology on FSPed Mg-Micro Al_2O_3 workpiece using tool shoulder diameter of (a) 20 mm, (b) 18 mm, (c) 15 mm, (d) 12 mm, and (e) 9 mm

In Figure 4(d), the tool shoulder with a 12 mm diameter presents the FSP zone line, which is the most stable and even with the smallest tunnel defect that is closer to no defect. Moreover, the material flow in FSPed Mg-Micro Al_2O_3 is more homogeneous compared to the other samples due to the strong and hard particles reinforced, which inhibits the FSP stirring of material [27]. This shows that the tool shoulder diameter of 12 mm is the most suitable as the current FSP tool shoulder parameter to process Mg-Micro Al_2O_3. Lastly, Figure 4 (e) presents the tool shoulder diameter of 9 mm produces the smoothest and shiniest FSP zone line with no tunnel defect. Nevertheless, the edge was not fully processed due to the narrow contact area from the small diameter of the tool shoulder, which produced less frictional heat [28]. Thus, they are unable to properly deform the material on the workpiece. Additionally, a smaller shoulder diameter forms several defects in the matrix composite [29].

Hardness on FSPed Mg AZ91A/Al_2O_3

The hardness measurements on the FSPed Mg-Micro Al_2O_3 were performed on the face of weld, at locations 1-6, as shown in Figure 5. The hardness readings of FSPed Mg-Micro Al_2O_3 by using different shoulder diameters on six different points were recorded and tabulated in Table 3. Then, the hardness on six different points for each sample was calculated into average hardness. The hardness readings of FSPed Mg-Micro Al_2O_3 by using different shoulder diameters on six different points were illustrated in Figure 6 through a line graph to analyze the trend changes of hardness.

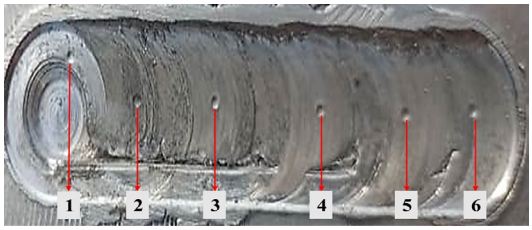

Figure 5. Location for hardness test points

Table 3. The hardness of FSPed Mg-Micro Al_2O_3 for different shoulder diameters at different locations

Shoulder diameter, D (mm)	Hardness (HRB)						
	1	2	3	4	5	6	Average
20	79	71	69	76	68	67	72
18	84	69	75	71	70	71	73
15	83	66	74	72	69	64	71
12	85	80	98	90	84	85	87
9	81	67	77	73	68	66	72

Figure 6 shows that the shoulder diameter of 12 mm has the highest average hardness which is 87 HRB compared to other shoulder diameters which have almost similar average hardness results. The maximum average hardness occurs due to the formation of fine and recrystallized grains [30] which can be seen in Figure 7(d). The hardness of FSPed Mg-Micro Al_2O_3 using a 12 mm shoulder diameter was significantly noticeable which the minimum hardness being 80 HRB at location 2 whereas the maximum hardness is 98 HRB at location 3. The same trend of hardness values from the first location to the sixth location between the shoulder diameter of 12 mm and 18 mm, which are 85, 80, 98, 90, 84 and 85 HRB and 84, 69, 75, 71, 70 and 71 HRB, respectively. In addition, the same trend of hardness values from the first location until the sixth location between the shoulder diameter of 9 mm and 15 mm which are 81, 67, 77, 73, 68 and 66 HRB and 83, 66, 74, 72, 69 and 64 HRB, respectively.

Focusing on the hardness for shoulder diameter 20 mm with 69 HRB, which is vice versa from the values for other shoulder diameters that increase at location 3, whereas the hardness for shoulder diameter 20 mm with 76 HRB, which is vice versa from the values for other shoulder diameters that decrease at location 4. This is due to the non-uniform distribution as well as an agglomeration of Al_2O_3 microparticles in the stirred zone [31]. Microparticles influence agglomeration to lower the total energy due to high surface area. Agglomeration also produces pores and enlarges the inter-particle spacing thus weakening the strength [32].

Overall, the increment in microhardness shows that the mechanical properties of FSPed Mg AZ91A were enhanced by the grain refinement and incorporation of Al_2O_3 microparticles. The decrement of the grain size that can be observed in Figure 7 causes the hardness enhancement following the Hall-Petch relationship, which monopolizes the strengthening of the grain and sub-grain boundary. Sanaty-Zadeh et al. [33] validated that the Hall-Petch relationship is the most influential aspect in strengthening. Besides, the Orowan strengthening mechanism owing to the uniformly dispersed microsized Al_2O_3 particles is another contributor to the improvement of the microhardness when fabricating surface composites [34]. An increase in hardness to a significant value is due to the higher inherent hardness (2500 kg/mm^2) of the reinforcement particles. Moreover, Guo et al. [35] demonstrated that the contribution of Orowan strengthening was roughly four times better than the improvement by grain refinement. The dispersed reinforcing particles recover the ductility of FSPed Mg-Micro Al_2O_3 composites by expanding the dislocation storage capability [36].

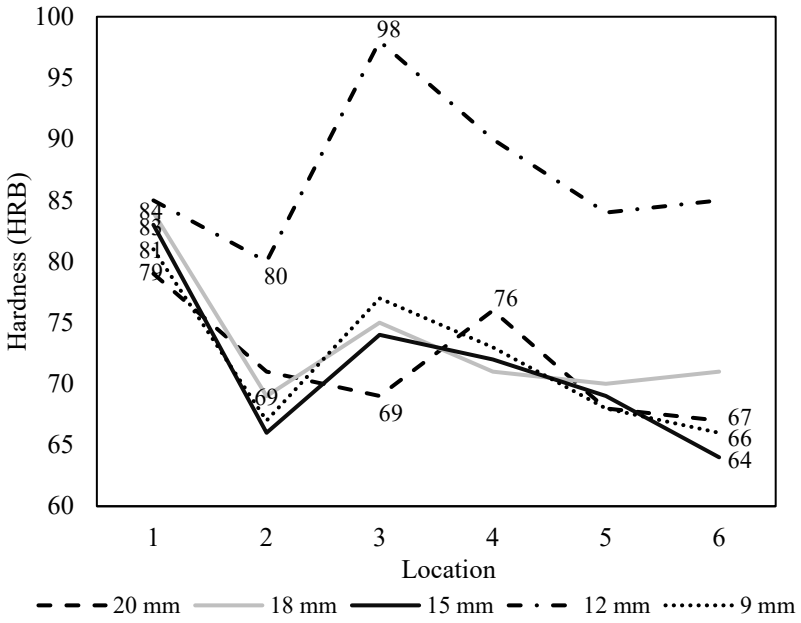

Figure 6. The hardness of FSPed Mg-Micro Al_2O_3 for different shoulder diameters at different locations

Microstructure Observations on FSPed Mg AZ91A/Al_2O_3

The mechanical properties depend on the grain size of the stirred zone. The results in Figure 7 show the grain size using a 12-mm diameter tool shoulder when friction stir processing Mg-Micro Al_2O_3 produced finer grain. Figure 7(a), 7(b), 7(c) and 7(e) have almost similar grain size and structure (red circle) but are larger when compared to the grain size in Figure 7(d) as it consists of finer and smallest grain size. The smaller grain size indicates that the grain is in the recrystallization state, which will create new grains hence giving rise to the hardness of the FSPed Mg-Micro Al_2O_3. The smaller the grain size, the greater the hardness of Mg-Micro Al_2O_3. Figure 7(d) has more colonies of finer grains which give better mechanical properties [37]. The grain is refined considering the continuous dynamic recrystallization from heavy plastic deformation while FSP [38]. Fine recrystallized grains occurred in Figure 7(d) due to the thermo-mechanical action of the tool shoulder and forging force [39] as well as the stirring action of the tool pin forces the thermo-mechanically process causing dynamic recrystallization, which shrinks the grain, enlarges the dislocations and ultimately enhances the microhardness.

Synthesized Al_2O_3 microparticles were almost agglomerated to form clusters of microsized reinforcements [40] at grain boundaries in the initial composite. The initial clusters were broken up thus, create a high number of misoriented grain boundaries, whereas Al_2O_3 microparticles were distributed more uniformly in the FSPed Mg-Micro Al_2O_3 composite, as shown in Figure 7(d). A high proportion of microparticles dispersed uniformly due to the substantial stirring during FSP. Furthermore, the nucleation of new recrystallized grains can be triggered by the presence of well-dispersed microsized Al_2O_3 particles. The Al_2O_3 particles in stirred zone act as nucleation spots for preexisting grain boundaries or deformation chain terminals, also known as new dislocation-free grains to be produced and cause non-homogeneous local deformation, which help the grain to scatter [36], [41]. The growth of fine nuclei started later; thus a microstructure showing fine equiaxed grains is produced.

Another finding reported that a high quantity of dislocated grains was formed from the applied strain during FSP and inhibited the growth of recrystallized grains [42]. Hence, the grain size was reduced in the stirred zone. A high free dislocation density along with fine cell formation are the components of the strain-induced build-up of stored strain energy and function as the driving force in initiating recrystallization. The high temperature from deformation leads to high stored strain energy due to the large area in the grain boundary of fine grain microstructure. Approaching the lowest level of stacking fault energy, the cross-slip and climb processes of dynamic recovery was retarded. Stable grain nuclei were produced at diverse locations, thus, the growth of new fine grains begins [43]. The newly produced grains deform as they grow. The driving force for grain growth is weakened by the build-up of stored strain energy yet raises the recurrence of new grains to be initiated [44].

An essential factor in controlling the number of grain growth is the distribution of the second-phase particles on the grain boundaries (Zener pinning). The pinning effect of dispersed reinforced particles as the grains grow restricts the movement of dislocations [45] and shifts grain boundaries just as the critical grain size is attained, so the grain growth slows down. The small particle size of Al_2O_3 particles steps up the pinning of the grain boundary resulting in grain refinement and larger grain numbers [43]. However, Shafiei-Zarghani et al. [46] related the size of grains observed from the FSP experiment with the Zener limiting grain size (d_z) in FSPed AA6082/Al_2O_3 composites. On the surface composite, the grain size discovered was larger than d_z as local clustering at a certain level is unavoidable, including some particles that are unable to pin the migration of grain boundary effectively. In a single pass of FSP, the non-uniform dispersion of reinforced particles creates a high difference between the composite's grain size and d_z. On the contrary, Ghasemi

Kahrizsangi et al. [47] found that the size of grains is consistent with the d_z. Other than that, grains were refined into a smaller size when TiC particles were incorporated compared to no second-phase particle added into the material.

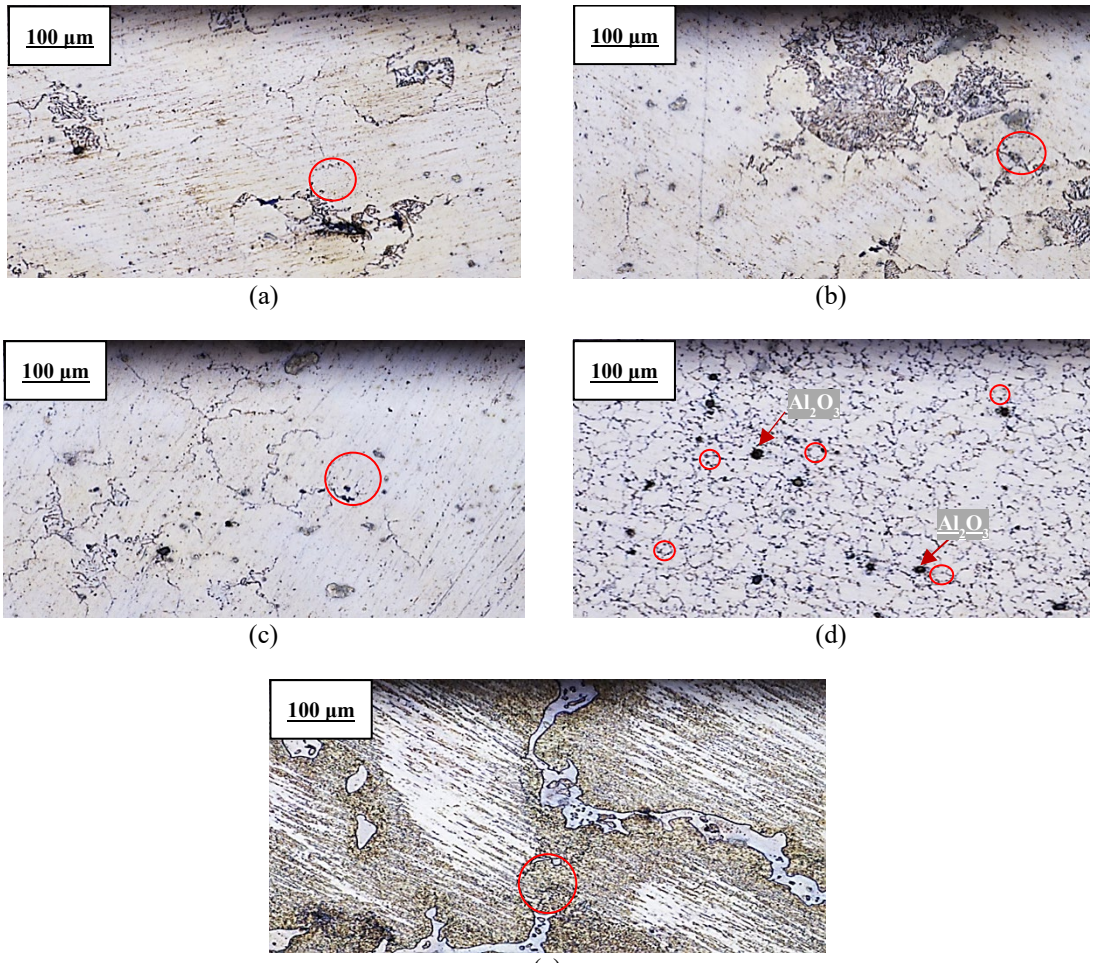

Figure 7. The microstructure observations on FSPed Mg-Micro Al_2O_3 workpiece using tool shoulder diameter of (a) 20 mm (b) 18 mm (c) 15 mm (d) 12 mm and (e) 9 mm

CONCLUSIONS

An investigation has been made of the effects on the mechanical properties of FSPed Mg AZ91A reinforced with aluminium oxide. Some concluding observations from the investigation are as follows.

i. The shoulder-to-pin diameter (D/d) ratio, along with the relevant machining parameter setup, influences the deformation of the FSPed Mg AZ91A reinforced with Al_2O_3.
ii. The lower the (D/d) ratio, the fewer the defects found on Mg-Micro Al_2O_3 composites as well as, the shinier surface finish produced.
iii. Fine distribution of Al_2O_3 reinforcement within the matrix using a 12 mm shoulder diameter was observed, which has a considerable effect on the hardness, with the highest average hardness value at 87 HRB.
iv. The grain structure for the stirred zone of Mg-Micro Al_2O_3 using the shoulder diameter of 12 mm is the smallest when compared to the other tool's shoulder diameters.
v. The shoulder diameter of 12 mm was the best tool parameter when using the setup machining parameter of 1040 rpm spindle speed and 17 mm/min traverse speed as it produces fewer defects and fine recrystallized grains.

Other implementations of shoulder diameter using different tool geometry should be considered and experimented with for future prospects to achieve a better surface finish and more uniform distribution of Al_2O_3 in Mg AZ91A.

ACKNOWLEDGEMENT

The authors gratefully appreciate Universiti Malaysia Pahang, the Ministry of Higher Education Malaysia and the Ministry of Science, Technology and Innovation (MOSTI) for providing support in technical and financial aspects through the Fundamental Research Grant Scheme FRGS/1/2019/TK03/UMP/02/17 (RDU 1901140).

REFERENCES

[1] Z. Hamedon, Y. Abe, K.-I. Mori, and N. Nakagawa, "Thickened holes edge including compressed rollover for improving tensile fatigue strength of thick sheet," *Procedia Manuf.*, vol. 15, pp. 612–618, 2018.

[2] P. Cavaliere, "Mechanical properties of friction stir processed 2618/Al2O3/20p metal matrix composite," *Compos. Part A*, vol. 36, no. 12, pp. 1657-1665, 2005.

[3] J. Stephens, "High temperature metal matrix composites for future aerospace systems," In Proc. of 24th Joint Propulsion Conference, October 1987, p. 3059.

[4] Z. Zulkfli, and N. Fatchurrohman, "Advancement in friction stir processing on magnesium alloys," *IOP Conf. Ser.: Mater. Sci. Eng.*, vol. 1092, no. 1, p. 012006, 2021.

[5] B. R. Sunil, G. P. K. Reddy, H. Patle, and R. Dumpala, "Magnesium based surface metal matrix composites by friction stir processing," *J. Magnes. Alloy.*, vol. 4, no. 1, pp. 52–61, 2016.

[6] K. Colligan, "Material flow behavior during friction stir welding of aluminum," *Weld. J.*, vol. 78, pp. 229-s, 1999.

[7] T. U. Seidel, and A. P. Reynolds, "Visualization of the material flow in AA2195 friction-stir welds using a marker insert technique," *Metall. Mater. Trans. A*, vol. 32, no. 11, pp. 2879-2884, 2001.

[8] D. Yadav, and R. Bauri, "Effect of friction stir processing on microstructure and mechanical properties of aluminium," *Mater. Sci. Eng. A*, vol. 539, pp. 85–92, 2012.

[9] A. Ali, X. An, C. A. Rodopoulos, M. W. Brown, P. O'hara *et al.*, "The effect of controlled shot peening on the fatigue behaviour of 2024-T3 aluminium friction stir welds," *Int. J. Fatigue*, vol. 29, no. 8, pp. 1531-1545, 2007.

[10] G. Vedabouriswaran, and S. Aravindan, "Development and characterization studies on magnesium alloy (RZ 5) surface metal matrix composites through friction stir processing," *J. Magnes. Alloy.*, vol. 6, no 2, pp. 145–163, 2018.

[11] N. A. Wahab, N. Fatchurrohman, and Z. Zulkfli, "Investigation on the effect of different friction stir machining tools shape on the mechanical properties of magnesium alloy work piece," *IOP Conf. Ser.: Earth Environ. Sci.*, vol. 700, no. 1, p. 012003, 2021.

[12] R. Palanivel, P. K. Mathews, N. Murugan, and I. Dinaharan, "Effect of tool rotational speed and pin profile on microstructure and tensile strength of dissimilar friction stir welded AA5083-H111 and AA6351-T6 aluminum alloys," *Mater. Des.*, vol. 40, pp. 7-16, 2012.

[13] M. Zohoor, M. B. Givi, and P. Salami, "Effect of processing parameters on fabrication of Al–Mg/Cu composites via friction stir processing," *Mater. Des.*, vol. 39, pp. 358-365, 2012.

[14] R. S. Mishra, and Z. Y. Ma, "Friction stir welding and processing," *Mater. Sci. Eng. R.*, vol. 50, no. 1-2, pp. 1-78, 2005.

[15] V. Sharma, U. Prakash, and B. V. M. Kumar, "Surface composites by friction stir processing: A review," *J. Mater. Process. Technol.*, vol. 224, pp. 117–134, 2015.

[16] A. Janeczek, J. Tomków, and D. Fydrych, "The influence of tool shape and process parameters on the mechanical properties of AW-3004 aluminium alloy friction stir welded joints," *Materials*, vol. 14, no. 3244, pp. 1–15, 2021.

[17] N. Parumandla, and K. Adepu, "Effect of tool shoulder geometry on fabrication of Al/Al_2O_3 surface nano composite by friction stir processing," *Part. Sci. Technol.*, vol. 38, no. 1, pp. 121–130, 2020.

[18] B. R. Powell, P. E. Krajewski, and A. A. Luo, "Magnesium alloys for lightweight powertrains and automotive structures," In *Woodhead Publishing Series in Composites Science and Engineering*, P.K. Mallick, Ed. Woodhead Publishing, 2010, pp. 114-173.

[19] C. D. Marini, N. Fatchurrohman, and Z. Zulkfli, "Investigation of wear performance of friction stir processed aluminium metal matrix composites," *Mater. Today: Proc.*, vol. 46, pp. 1740-1744, 2021.

[20] G. F. Vander Voort, "Metallography of magnesium and its alloys," *Metall. Ital.*, vol. 4, no. 2, pp. 37–41, 2015.

[21] E. B. F. Lima, J. Wegener, C. Dalle Donne, G. Goerigk, T. Wroblewski *et al.*, "Dependence of the microstructure, residual stresses and texture of AA 6013 friction stir welds on the welding proces," *Int. J. Mater. Res.*, vol. 94, no. 8, pp. 908-915, 2003.

[22] A. A. N. A. Oosterkamp, L. D. Oosterkamp, and A. Nordeide, "Kissing bond phenomena in solid-state welds of aluminum alloys," *Weld. J.*, vol. 83, no. 8, pp. 225-S, 2004.

[23] Y. S. Sato, Y. Sugiura, Y. Shoji, S. H. C. Park, H. Kokawa, and K. Ikeda, "Post-weld formability of friction stir welded Al alloy 5052," *Mater. Sci. Eng. A.,* vol. 369, no. 1-2, pp. 138-143, 2004.

[24] J. Gandra, R. Miranda, P. Vilaca, A. Velhinho, and J. P. Teixeira, "Functionally graded materials produced by friction stir processing," *J. Mater. Process. Technol.*, vol. 211, no. 11, pp. 1659-1668, 2011.

[25] S. Kalidass, S. Gnanasekaran, A. R. Akilesh, N. T. Gokul Kumar, M. Aswin, C. Rajendran, and T. Sonar, "Investigation of shoulder diameter to sheet thickness (D/T) ratio on tensile properties friction stir welded AA2014-T6 aluminum alloy joints," *Adv. Mater. Process. Technol.*, vol. 8, no. 3, pp. 3440-3453, 2022.

[26] N. Gangil, S. Maheshwari, and A. N. Siddiquee, "Surface nanocomposite fabrication on AA6063 aluminium alloy using friction stir processing: an investigation into the effect of the tool-shoulder diameter on the composite microstructure," *Mater. Technol.*, vol. 52, no. 1, pp. 77–82, 2018.

[27] M. Azizieh, A. N. Larki, M. Tahmasebi, M. Bavi, E. Alizadeh *et al.*, "Wear behavior of AZ31/Al 2 O 3 magnesium matrix surface nanocomposite fabricated via friction stir processing," *J. Mater. Eng. Perform.*, vol. 27, no. 4, pp. 2010-2017, 2018.

[28] W. M. Thomas, and E. D. Nicholas, "Friction stir welding for the transportation industries," *Mater. Des.*, vol. 18, no. 4-6, pp. 269-273, 1997.

[29] K. Elangovan, and V. Balasubramanian, "Influences of tool pin profile and tool shoulder diameter on the formation of friction stir processing zone in AA6061 aluminium alloy," *Mater. Des.*, vol. 29, no. 2, pp. 362-373, 2008.

[30] C. Rajendran, K. Srinivasan, V. Balasubramanian, H. Balaji, and P. Selvaraj, "Feasibility study of FSW, LBW and TIG joining process to fabricate light combat aircraft structure," *Int. J. Lightweight Mater. Manuf.*, vol. 4, pp. 480–490, 2021.

[31] Mohsen Barmouz, M. K. Besharati Givi, and J. Seyfi, "On the role of processing parameters in producing Cu/SiC metal matrix composites via friction stir processing: investigating microstructure, microhardness, wear and tensile behavior," *Mater. Charact.*, vol. 62, no. 1, pp. 108–117, 2011a.

[32] S.C. Tjong, "Novel nanoparticle-reinforced metal matrix composites with enhanced mechanical properties," *Adv., Eng. Mater.*, vol. 9, no. 8, pp. 639-652, 2007.

[33] A. Sanaty-Zadeh, "Comparison between current models for the strength of particulate-reinforced metal matrix nanocomposites with emphasis on consideration of Hall–Petch effect," *Mater. Sci. Eng. A.*, vol. 531, pp. 112-118, 2012.
[34] M. Narimani, B. Lotfi, and Z. Sadeghian, "Evaluation of the microstructure and wear behaviour of AA6063-B4C/TiB2 mono and hybrid composite layers produced by friction stir processing," *Surf. Coat. Technol.*, vol. 285, pp. 1-10, 2016.
[35] J. F. Guo, J. Liu, C. N. Sun, S. Maleksaeedi, G. Bi, M. J. Tan, and J. Wei, "Effects of nano-Al2O3 particle addition on grain structure evolution and mechanical behaviour of friction-stir-processed Al," *Mater. Sci. Eng. A.*, vol. 602, pp. 143-149, 2014.
[36] S. M. Ma, P. Zhang, G. Ji, Z. Chen, G. A. Sun *et al.*, "Microstructure and mechanical properties of friction stir processed Al-Mg-Si alloys dispersion-strengthened by nanosized TiB2 particles," *J. Alloys Compd.*, vol. 616, pp. 128–136, 2014.
[37] M. A. Khattak, S. Zaman, M. N. Tamin, S. Badshah, S. Mushtaq, and A. A. B. Omran, "Effect of welding phenomenon on the microstructure and mechanical properties of ferritic stainless steel-A review," *J. Adv. Res. Mater. Sci.*, vol. 32, no. 1, pp. 13-31, 2017.
[38] D. Yadav, and R. Bauri, "Processing, microstructure and mechanical properties of nickel particles embedded aluminium matrix composite," *Mater. Sci. Eng. A.,* vol. 528, no. 3, pp. 1326–1333, 2011.
[39] C. Rajendran, K. Srinivasan, V. Balasubramanian, H. Balaji, and P. Selvaraj, "Evaluation of load-carrying capabilities of friction stir welded, TIG welded and riveted joints of AA2014-T6 aluminium alloy," *Aircr. Eng. Aerosp. Technol.,* vol. 91, no. 9, pp. 1238–1244, 2019.
[40] M. Sharifitabar, A. Sarani, S. Khorshahian, and M. S. Afarani, "Fabrication of 5052Al/Al2O3 nanoceramic particle reinforced composite via friction stir processing route," *Mater. Des.*, vol. 32, no. 8-9, pp. 4164-4172, 2011.
[41] A. Dolatkhah, P. Golbabaei, M. K. Besharati Givi, and F. Molaiekiya, "Investigating effects of process parameters on microstructural and mechanical properties of Al5052/SiC metal matrix composite fabricated via friction stir processing," *Mater. Des.*, vol. 37, pp. 458–464, 2012.
[42] F. J. Humphreys, and M. Hatherly, *Recrystallization and related annealing phenomena*, Elsevier, 2012.
[43] M. Barmouz, P. Asadi, M. K. Besharati Givi, and M. Taherishargh, "Investigation of mechanical properties of Cu/SiC composite fabricated by FSP: effect of SiC particles' size and volume fraction," *Mater. Sci. Eng. A.,* vol. 528, pp. 1740–1749, 2011.
[44] T. R. McNelley, S. Swaminathan, and J. Q. Su, "Recrystallization mechanisms during friction stir welding/processing of aluminum alloys," *Scr. Mater.*, vol. 58, no. 5, pp. 349-354, 2008.
[45] A. Shafiei-Zarghani, S. F. Kashani-Bozorg, and A. Z. Hanzaki, "Wear assessment of Al/Al2O3 nano-composite surface layer produced using friction stir processing," *Wear*, vol. 270, no. 5–6, pp. 403–412, 2011.
[46] A. Shafiei-Zarghani, S. F. Kashani-Bozorg, and A. Zarei-Hanzaki, "Microstructures and mechanical properties of Al/Al2O3 surface nano-composite layer produced by friction stir processing," *Mater. Sci. Eng. A.,* vol. 500, no. 1-2, pp. 84-91, 2009.
[47] A. Ghasemi-Kahrizsangi, and S. F. Kashani-Bozorg, "Microstructure and mechanical properties of steel/TiC nano-composite surface layer produced by friction stir processing," *Surf. Coat. Technol.*, 209, pp. 15-22, 2012.